ENVIRONMENTAL RESEARCH
CLIMATE

PAPER • OPEN ACCESS

Meteorological and geographical factors associated with dry lightning in central and northern California

To cite this article: Dmitri A Kalashnikov *et al* 2022 *Environ. Res.: Climate* **1** 025001

ENVIRONMENTAL RESEARCH
CLIMATE

CrossMark

OPEN ACCESS

RECEIVED
6 May 2022

REVISED
5 July 2022

ACCEPTED FOR PUBLICATION
27 July 2022

PUBLISHED
8 August 2022

PAPER

Meteorological and geographical factors associated with dry lightning in central and northern California

Dmitri A Kalashnikov[1,*], **John T Abatzoglou**[2], **Nicholas J Nauslar**[3], **Daniel L Swain**[4,5,6], **Danielle Touma**[7] and **Deepti Singh**[1]

[1] School of the Environment, Washington State University, Vancouver, WA, United States of America
[2] Management of Complex Systems Department, University of California, Merced, Merced, CA, United States of America
[3] Predictive Services, Bureau of Land Management, National Interagency Fire Center, Boise, ID, United States of America
[4] Institute of the Environment and Sustainability, University of California, Los Angeles, Los Angeles, CA, United States of America
[5] Capacity Center for Climate and Weather Extremes, National Center for Atmospheric Research, Boulder, CO, United States of America
[6] The Nature Conservancy of California, Sacramento, CA, United States of America
[7] Climate and Global Dynamics Laboratory, National Center for Atmospheric Research, Boulder, CO, United States of America
[*] Author to whom any correspondence should be addressed.

E-mail: dmitri.kalashnikov@wsu.edu

Keywords: lightning, wildfires, California, clustering, meteorology

Supplementary material for this article is available online

Abstract

Lightning occurring with less than 2.5 mm of rainfall—typically referred to as 'dry lightning'—is a major source of wildfire ignition in central and northern California. Despite being rare, dry lightning outbreaks have resulted in destructive fires in this region due to the intersection of dense, dry vegetation and a large population living adjacent to fire-prone lands. Since thunderstorms are much less common in this region relative to the interior West, the climatology and drivers of dry lightning have not been widely investigated in central and northern California. Using daily gridded lightning and precipitation observations (1987–2020) in combination with atmospheric reanalyses, we characterize the climatology of dry lightning and the associated meteorological conditions during the warm season (May–October) when wildfire risk is highest. Across the domain, nearly half (∼46%) of all cloud-to-ground lightning flashes occurred as dry lightning during the study period. We find that higher elevations (>2000 m) receive more dry lightning compared to lower elevations (<1000 m) with activity concentrated in July-August. Although local meteorological conditions show substantial spatial variation, we find regionwide enhancements in mid-tropospheric moisture and instability on dry lightning days relative to background climatology. Additionally, surface temperatures, lower-tropospheric dryness, and mid-tropospheric instability are increased across the region on dry versus wet lightning days. We also identify widespread dry lightning outbreaks in the historical record, quantify their seasonality and spatial extent, and analyze associated large-scale atmospheric patterns. Three of these four atmospheric patterns are characterized by different configurations of ridging over the continental interior and offshore troughing. Understanding the meteorology of dry lightning across this region can inform forecasting of possible wildfire ignitions and is relevant for assessing changes in dry lightning and wildfire risk in climate projections.

1. Introduction

Wildfires are a growing threat in California as the climate continues to warm. While human-caused wildfire ignitions predominate in southern California, lightning-caused fires are more prevalent in the northern half of the state, particularly over mountainous terrain (Show and Kotok 1923, Komarek 1967, Balch *et al* 2017, Brey *et al* 2018, Keeley and Syphard 2018, Chen and Jin 2022). Summertime lightning outbreaks accompanied by little or no rainfall (hereafter, 'dry lightning') pose a threat for wildfire ignition where they align with flammable fuels. Unlike human-caused fires that originate in a single location, lightning outbreaks can strike multiple locations and start numerous simultaneous wildfires (Court 1960, Komarek 1967, Bartlein *et al* 2008, Wallmann *et al* 2010, Miller *et al* 2012). Widespread thunderstorms with dry lightning produced some of the largest and longest-lasting wildfires in recent decades in California, notably in 1987 (Duclos *et al* 1990), 2008 (Wallmann *et al* 2010), and 2020 (Keeley and Syphard 2021).

Despite its importance for wildfire ignition, few studies have explored dry lightning in central and northern California. Previous studies of summertime lightning in the western United States have omitted lower-elevation areas within this region due to small sample sizes of lightning activity (e.g. Easterling and Robinson 1985, Abatzoglou *et al* 2016, Kalashnikov *et al* 2020). Case studies have investigated the meteorology of notable dry lightning outbreaks to inform operational forecasting on short timescales (e.g. Wallmann *et al* 2010, Nauslar *et al* 2013). van Wagtendonk and Cayan (2008) developed a climatology of lightning and associated meteorological patterns for California, but without a specific focus on dry lightning. A systematic climatology of dry lightning and associated meteorological conditions has thus not yet been developed for this region.

This study leverages three decades of gridded cloud-to-ground lightning and precipitation data (1987–2020) to compile the first long-term climatology of dry lightning for central and northern California. We utilize atmospheric reanalysis data to quantify the meteorological conditions that produce dry lightning and examine their differences compared to 'wet' lightning. Due to their ability to produce widespread and costly wildfire outbreaks, we also analyze historical widespread dry lightning episodes and identify associated large-scale atmospheric patterns. As lightning climatology is strongly linked to topography in California (van Wagtendonk and Cayan 2008), we additionally explore the influence of elevation on dry lightning across this region. Understanding the characteristics and meteorological drivers of dry lightning is critical for anticipating fire ignitions in the present climate and for fully characterizing the changing risk of wildfires, including multiple fire ignitions, with ongoing and projected warming and drying in the region (Abatzoglou and Williams 2016, Goss *et al* 2020, Parks and Abatzoglou 2020).

2. Materials and methods

2.1. Study domain

In this analysis, we focus on the warm season (May–October) due to the co-occurrence of dry lightning and seasonally dry vegetation that enhances wildfire risk. Our study domain encompasses the North Coast, Central Coast, and Sierra Nevada regions defined in Williams *et al* (2019) from Bailey's ecoregion sections and includes the Central Valley to form a spatially contiguous region (figure 1(A)). We focus on this region because of the relatively large tree cover and vegetation fraction and large wildfire burned areas associated with lightning relative to southern California, where humans are the major source of historical wildfire ignitions and burned area (figures 1(B), (C) and S.1) (Brey *et al* 2018, Keeley and Syphard 2018). Our domain excludes the western Great Basin for two primary reasons. *First*, the lightning-wildfire relationship differs in the Great Basin due to differences in both climate and vegetation composition, where both dry lightning flashes and lightning-ignited wildfires are climatologically more frequent compared to our domain (Abatzoglou *et al* 2016, Brey *et al* 2018), yet sparser fuels typically prevent most fires from growing large (Williams *et al* 2019). Outside of the agricultural lands of the Central Valley, most of our domain contains substantial tree cover (figure 1(C)), which provides additional fuel when compared to shrubs and herbaceous fuels common to other parts of the state (figure S.1) and increases the risk of sustained wildfire ignition resulting from a cloud-to-ground lightning flash (Hantson *et al* 2022). *Second*, the North American Monsoon brings moisture to the eastern fringe of California, favoring convection and substantially more lightning activity in the Great Basin (figure 1(D)), whereas our domain usually remains dry and free of lightning during such events. Despite being relatively rare in the historical record, our domain has experienced multiple dry lightning outbreaks over the past three decades that have led to numerous simultaneous wildfire ignitions and subsequently to large areas burned (e.g. in August 2020)—threatening the region's population, infrastructure, and air quality (Podschwit and Cullen 2020, Kalashnikov *et al* 2022). Due to its potentially outsized societal and ecological impacts, we focus our analysis on dry lightning in this distinct domain.

2.2. Datasets

Daily-gridded cloud-to-ground lightning flash totals ($0.1^{\circ} \times 0.1^{\circ}$, 1987–2020) from the National Lightning Detection Network (NLDN) were sourced from the National Centers for Environmental Information Severe Weather Data Inventory (www.ncei.noaa.gov/pub/data/swdi/database-csv/v2/). Daily precipitation amounts

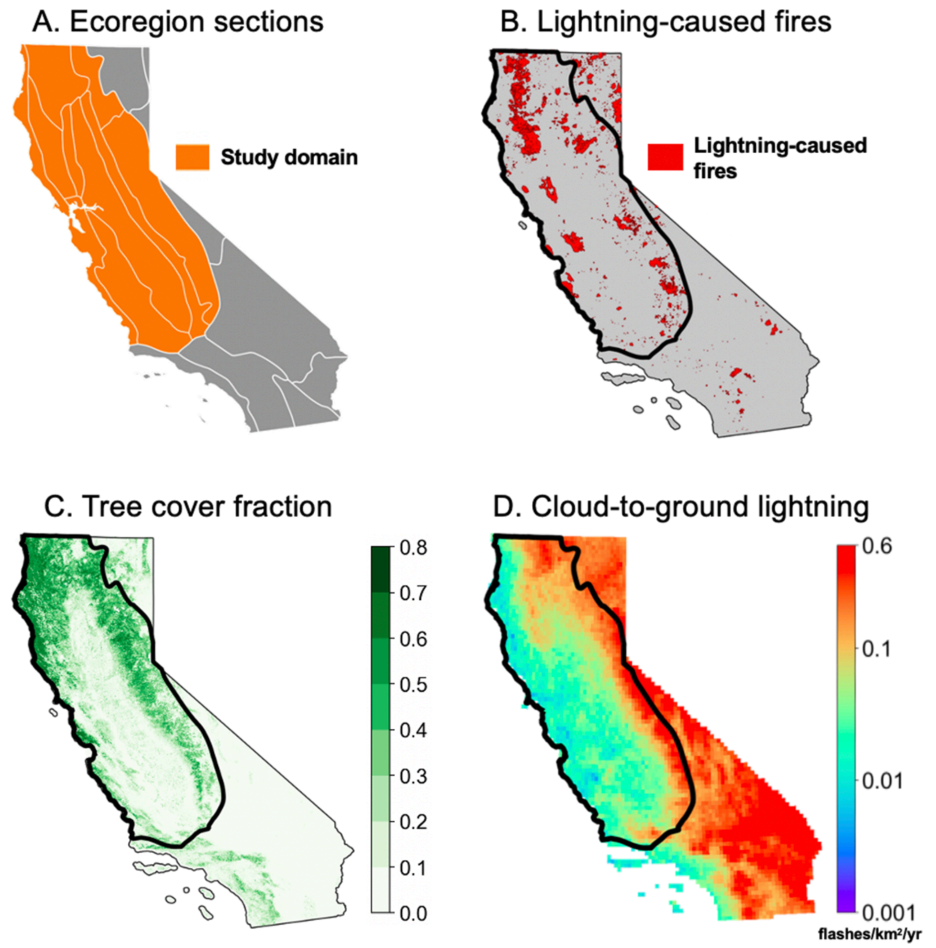

Figure 1. (A) The study domain (orange) comprised of Bailey's ecoregion sections. (B) Lightning-caused wildfire perimeters (red) from the California Department of Forestry and Fire Protection (CAL FIRE) for May–October 1987–2020. (C) Tree cover fraction from the Moderate Resolution Imaging Spectroradiometer at each 250 m grid cell. (D) Density of cloud-to-ground lightning flashes averaged over May–October 1987–2020 (flashes km^{-2} yr^{-1}). Study outline is shown in black in (A, C and D). Note that values in (D) are presented on a base-10 logarithmic scale. Maps were created using the QGIS open-source software.

were obtained from the widely used, high-resolution (4 km) gridMET dataset (Abatzoglou 2013) and interpolated to the 0.1° grid of the NLDN dataset using bilinear interpolation from the *GeoCAT-comp* Python package (VAST 2021). Other meteorological variables are from the European Centre for Medium-Range Weather Forecasts Reanalysis v5 (ERA5) at a 0.25° resolution (Hersbach *et al* 2020). For analyzing the influence of elevation on dry lightning, grid cell elevations were calculated using surface geopotential from ERA5 at a 0.1° resolution (www.ecmwf.int/en/era5-land).

For delineating the study domain, polygons of Bailey's ecoregion sections were sourced from the United States Geological Survey (USGS) (www.sciencebase.gov/catalog/item/54244abde4b037b608f9e23d). Tree cover and vegetation fraction over the domain (as of 2020; 250 m resolution) are from the Moderate Resolution Imaging Spectroradiometer's Vegetation Continuous Fields database (MOD44B) sourced from the USGS Land Processes Distributed Active Archive Center (https://lpdaacsvc.cr.usgs.gov/appeears/). The vegetation fraction was computed at each grid cell using the 'Percent_NonVegetated' dataset from MOD44B.

Wildfire information for May–October 1987–2020 was obtained from the multi-agency 'Fire Perimeters through 2020' dataset, sourced from the California Department of Forestry and Fire Protection (CAL FIRE) Fire and Resource Assessment Program (https://frap.fire.ca.gov/). This dataset excludes timber fires <4 ha, brush fires <12 ha, and grass fires <121 ha when reported by CAL FIRE, and all fires <4 ha when reported by the United States Forest Service, and assigns 19 possible fire causes including 'Lightning'. Any fires with perimeters intersecting the study domain boundary were considered part of the domain, and their final burned areas included herein. A total of 5479 fires were reported in the study domain, representing 6373 876 ha area burned between 1987 and 2020. Of these, 1562 were officially categorized as lightning-caused fires (∼28.5%) that accounted for nearly half of the total burned area (∼49.3%).

2.3. Dry lightning definition

We define a dry lightning day as any cloud-to-ground lightning detection synchronous with <2.5 mm (<0.10 inches) accumulated precipitation, using NLDN lightning and gridMET precipitation data. Daily rainfall below 2.5 mm is typically considered insufficient to prevent sustained fire ignition resulting from associated lightning strokes. This precipitation threshold is used operationally by the National Oceanic and Atmospheric Administration/National Weather Service Storm Prediction Center (www.spc.noaa.gov/exper/dryt/) and has been widely used in previous studies of dry lightning (e.g. Rorig and Ferguson 1999, Dowdy and Mills 2012a, Abatzoglou *et al* 2016, Dowdy 2020).

GridMET daily total precipitation is reported from midnight-midnight local time each calendar day whereas NLDN reported daily lightning totals are binned from 5 PM–5 PM local time. To account for the difference in the temporal aggregation of these datasets, we consider accumulated precipitation over two consecutive calendar days overlapping with the lightning data (e.g. from midnight-midnight local time on both calendar days). While this is a conservative approach less likely to falsely identify dry lightning, inclusion of a second calendar day could increase the two day accumulated precipitation beyond 2.5 mm, thereby not capturing dry lightning occurrence if either calendar day accumulated <2.5 mm of precipitation coincident with a cloud-to-ground flash. We test the sensitivity of our approach by using daily NLDN lightning data binned from midnight-midnight local time for 2017–19 acquired from the Western Regional Climate Center (https://wrcc.dri.edu/). Daily dry lightning extents from these datasets show substantial agreement ($r = 0.84$, $P < 0.05$, figure S.2), indicating that our approach reasonably captures dry lightning climatology in this region. Longer-term lightning data at higher temporal resolution is not yet publicly available and the costs of obtaining this data are prohibitive.

2.4. Dry lightning characteristics

We compile a climatology of dry lightning across the domain and compute the fraction of cloud-to-ground lightning flashes that were dry at each 0.1° grid cell ('*dry lightning fraction*'), further stratifying this climatology by month and by elevation zone. We define *dry lightning spatial extent* as the percentage of grid cells in our domain that experience dry lightning on a given day. *Widespread dry lightning days* are defined as days that have dry lightning spatial extents exceeding 6.1% ($\sim$15 200 km^2, $n = 124$ days), which represents the 95th percentile of these extents across the 34 year record. We also examine consecutive two day widespread dry lightning outbreaks as some events can last more than 24 h (Wallmann *et al* 2010). This approach additionally captures late-afternoon lightning outbreaks when lightning data might be split due to the temporal binning of the NLDN dataset.

Although not all widespread dry lightning outbreaks in our record resulted in large burned areas—owing to differences in the types of landscapes struck by lightning as well as antecedent climatic and biophysical controls on burned area (Barbero *et al* 2014, Abatzoglou *et al* 2016)—a portion of these outbreaks have nonetheless produced the largest and costliest lightning-ignited wildfire episodes in modern California history (Wallmann *et al* 2010, Keeley and Syphard 2021). To illustrate this, we estimate wildfire burned areas associated with the ten most widespread dry lightning days in the 34 year record from the CAL FIRE dataset. This is done by extracting all fires identified as lightning-caused with 'alarm dates' between -3 and $+3$ days from each of the ten most widespread dry lightning days, and aggregating their final burned areas. We do this to account for (a) the 5 PM–5 PM binning window of the lightning dataset overlapping two calendar dates of possible fire reports, (b) the prospect of 'holdover' fires, when fires are not detected for multiple days until they have grown sufficiently large for detection (Schultz *et al* 2019, MacNamara *et al* 2020), and (c) cases when the most widespread dry lightning day represents a multi-day sequence of dry lightning, when wildfire ignition and detection may have occurred several days prior to the most widespread dry lightning spatial extent of the multi-day episode.

2.5. Meteorological variables

Dry thunderstorms need three key ingredients to occur—mid-tropospheric moisture, a lifting mechanism, and a sufficiently dry lower-troposphere to evaporate the majority of rainfall before it reaches the ground (Rorig and Ferguson 1999, Rorig *et al* 2007, Wallmann *et al* 2010, Nauslar *et al* 2013). Lifting can be provided dynamically by transient cyclonic circulations (e.g. shortwave troughs) or thermodynamically through steep vertical temperature differences ('lapse rates'), or both (Rorig and Ferguson 1999, Wallmann *et al* 2010, Nauslar *et al* 2013). The cyclonic circulation around approaching shortwave troughs can additionally promote mid-tropospheric moisture transport to the region from either the Pacific Ocean or locations to the southeast where monsoonal moisture is more prevalent during the warm season (Wallmann *et al* 2010, Nauslar *et al* 2013).

We analyze several local meteorological variables that capture these conditions on dry lightning days at each 0.25° ERA5 grid cell with variable selection informed by literature. To capture atmospheric instability, the mid- ('MTLR') and upper-tropospheric lapse rates ('UTLR') are defined as vertical temperature differences ($^\circ$C km^{-1}) between 700–500 hPa and 500–300 hPa, respectively (Wallmann *et al* 2010, Nauslar *et al* 2013). Mid-tropospheric moisture is defined as the pressure-weighted specific humidity between 700 and 500 hPa ('$Q_{700-500}$') (Wallmann *et al* 2010, Nauslar *et al* 2013), computed from constituent ERA5 pressure levels at 50 hPa increments using the *MetPy* Python package (May *et al* 2021). To understand the degree to which large-scale weather patterns during dry lightning are transient and provide conditions potentially favorable for dynamic lifting, we examine mid-tropospheric wind speeds. While previous studies have utilized 700 hPa to analyze thunderstorm-relevant atmospheric flow (e.g. Soriano *et al* 2001, Bertram and Mayr 2004, Kalashnikov *et al* 2020), we analyze wind speed at 500 hPa ('UV_{500}') due to the elevated cloud bases known to exist with dry lightning (Rorig *et al* 2007, Nauslar *et al* 2013). Lower-tropospheric dryness is represented by the dewpoint depression (i.e. the difference between the temperature and dewpoint) at 850 hPa ('DD_{850}') following Rorig and Ferguson (1999). The 850 hPa dewpoint was calculated using *MetPy* from temperature and relative humidity fields provided by ERA5. Finally, we examine surface heating, represented by daily maximum temperatures ('$T_{\max}$'), as a proxy for near-surface instability and dryness.

The variables we have selected broadly describe the convective environment in which dry lightning occurs and are relatively straightforward to compute from ERA5 pressure-level data, making them useful for future studies evaluating climate model output. Although there are other variables such as convective available potential energy (CAPE) and Lifted Index that have been used to describe thunderstorm environments, we have not included them in our analysis for several reasons. *First*, due to the elevated cloud bases, surface- and lower troposphere-based convective parameters do not adequately describe the vertical instability profiles typically associated with dry lightning (Wallmann *et al* 2010). *Second*, although we considered using CAPE calculated from the most unstable air parcel in the lowest 300 hPa (e.g. 'Most Unstable CAPE'), to more accurately resolve elevated instability (Doswell and Rasmussen 1994, Rochette *et al* 1999), recent studies have noted substantial biases in modern atmospheric reanalyses relative to sounding data (e.g. Taszarek *et al* 2018). *Third*, the utility of computing Most Unstable CAPE as a climatological parameter over regional domains is unclear due to the widely varying vertical profiles of moisture and instability associated with individual dry lightning events (Wallmann *et al* 2010), making this variable more amenable to operational forecasting of individual events in combination with other diagnostics.

To understand meteorological characteristics unique to dry lightning days, we compare averages of all variables on dry lightning against 'wet lightning' days (cloud-to-ground lightning with $\geq$2.5 mm accumulated precipitation) (Rorig and Ferguson 1999, Bates *et al* 2017) and against local background climatology at each grid cell, computed using a running seven day mean across the 34 year record.

2.6. Identifying large-scale atmospheric patterns

Previous studies have shown that warm-season lightning outbreaks in different parts of California are associated with a set of distinct meteorological patterns (e.g. van Wagtendonk and Cayan 2008). To characterize the different types of large-scale atmospheric patterns observed on the 124 widespread dry lightning days, we perform k-means clustering (MacQueen 1967) on the associated 500 hPa geopotential heights ('Z_{500}') from ERA5. Clustering of atmospheric patterns is conducted over a larger region (25° N–50° N, 140° W–105° W) in order to capture large-scale atmospheric features potentially relevant for dry lightning meteorology over our study domain. We use a hybrid empirical-objective approach to select the k number of clusters (Grotjahn *et al* 2016, Detzer *et al* 2020). We analyzed multiple cluster arrangements over a range of cluster numbers ($k = 2$:8) and found that composite patterns constructed from four clusters (i.e. $k = 4$) sufficiently represent the diversity of atmospheric patterns associated with widespread dry lightning while minimizing overlap between patterns. Cluster representativeness was tested using 2D pattern correlation between each cluster's composite pattern and its constituent days. We note that a number of previous studies focused on this region have also used four large-scale patterns when characterizing the meteorology of flash flooding (Maddox *et al* 1980), lightning (van Wagtendonk and Cayan 2008), and heavy precipitation (Moore *et al* 2021).

At each NLDN grid cell, we calculate the likelihood of dry lightning occurring with each cluster's pattern relative to random chance. This is done by first dividing the number of dry lightning days at that grid cell associated with each cluster by the total number of dry lightning days recorded at that grid cell from all clusters. To account for the uneven binning of widespread dry lightning days between clusters, this fraction of dry lightning occurrences is then divided by the fraction of all widespread dry lightning days belonging to that cluster. This process produces a ratio where values >1 indicate an increased likelihood of dry lightning in that grid cell with that cluster's pattern compared to random chance alone. For each cluster, we compare the distributions of area-averaged meteorological variables (section 2.5) and assess statistical significance of differences from all other days using the Kolmogorov–Smirnov test.

3. Results and discussion

3.1. Climatology of dry lightning across elevation zones

The average number of annual dry lightning flashes varies substantially across the domain (figure 2(A)). Enhanced dry lightning activity is strongly tied to elevation across the region (figure 2(B), inset), with a larger mean number of flashes in the high-elevation zone (>2000 m) over the Sierra Nevada exceeding 0.5 flashes km^{-2} yr^{-1} (figure 2(A)). The greater density of dry lightning over the Sierra Nevada is consistent with studies that examined both dry lightning (e.g. Abatzoglou *et al* 2016) and total cloud-to-ground lightning (e.g. van Wagtendonk 1994, van Wagtendonk and Cayan 2008) over this region.

To assess the elevational dependence of dry lightning, we quantify dry lightning climatology across different elevation zones (figure 2(B)). The medium- (1000–2000 m) and high-elevation (>2000 m) zones show a pronounced dry lightning peak in July–August with only minimal activity in October (figure 2(B)). Dry lightning flash totals in the low-elevation zone (<1000 m) show less variability from June to September (figure 2(B), light brown). Further, while the high-elevation zone accounts for $\sim$50% of all dry lightning flashes across the domain in July, this proportion reduces to $\sim$26% in September (figure 2(B), dark brown). Conversely, the proportion of regionwide dry lightning occurring in the low-elevation zone increases from $\sim$14% in July to $\sim$39% in September (figure 2(B), light brown).

The dry lightning fraction is greater across the southern and western portions of the region, which comprise mainly low-elevation areas, and over the Sierra Nevada (figure 2(C)). In the high-elevation zone of the Sierra Nevada, $\sim$57% of all lightning flashes occurred as dry lightning in the 34 year record (figure 2(D), dark brown dashes) and this fraction exceeded 45% in all months except October (figure 2(D), dark brown bars). In the low-elevation zone, the average dry lightning fraction exceeds 40% in June–September (figure 2(D), light brown bars). Summed across the domain, nearly half ($\sim$46%) of all lightning flashes were dry in the 34 year record (figure 2(D), blue dashes).

Our finding of the large dry lightning fraction (>0.5) over the Sierra Nevada may be counterintuitive, as a deeper layer of sub-cloud dry air over low-elevation regions should increase the dry lightning fraction there relative to higher elevations. Over the Sierra Nevada, the relatively large dry lightning fraction could be indicative of a greater density of cloud-to-ground lightning flashes on dry lightning days versus wet lightning days, rather than a greater frequency of individual thunderstorms occurring as dry. Further, strong orographic lifting can produce convection over high terrain in the presence of less atmospheric moisture than would be required to produce convection over lower elevations (Tardy 2001), which may lead to increased incidence of dry thunderstorms over the Sierra Nevada. In addition, gridded precipitation datasets might not capture all convective precipitation which occurs over sparsely-gauged mountain regions (Abatzoglou *et al* 2016), resulting in a potential source of bias in the dry lightning fraction over the Sierra Nevada and other mountain ranges in the study domain. The smaller dry lightning fraction over the lower-elevations of the northern Sacramento Valley and adjacent foothills (figure 2(C)) could be indicative of the surface-based moisture convergence zone found here (Tardy 2002), which would increase the chance of rainfall exceeding 2.5 mm accompanying lightning.

3.2. Geographic variations in meteorological conditions on dry lightning days

The local meteorological conditions on dry lightning days also exhibit substantial variations across the domain (figure 3). On dry lightning days, 500 hPa wind speeds (UV_{500}) are strongest in the lower-elevation regions including the lowland San Francisco-Sacramento corridor of central California, exceeding 12 m s^{-1} (figure 3(A)). UV_{500} anomalies on dry lightning days are above background climatology in these areas, whereas they are >3 m s^{-1} below climatological values over the higher-elevation regions (figure 3(G)). This spatial pattern implies stronger mid-tropospheric steering flow and increased chances of dynamic lifting assisting convective development on dry lightning days at lower elevations compared to higher elevations, where convection can occur due to orographic lifting with lesser dependence on mid- and upper-tropospheric dynamics. Indeed, UV_{500} shows a robust negative correlation with elevation on dry lightning days across the domain (Spearman's rank correlation −0.86, $P < 0.05$; figure S.3(A)).

The UTLR is steepest over northern areas exceeding 7.3 °C km^{-1} on dry lightning days and reduces further south (figures 3(B) and S.4). Over most of the domain, UTLR is suppressed relative to background climatology (figure 3(H)). While UTLR exceeding 7.5 °C km^{-1} has been previously identified as an important ingredient of dry lightning over northern California (e.g. Wallmann *et al* 2010), our results suggest that lower UTLR values are sufficient to promote dry lightning over this region (figure 3(H)). In contrast, the MTLR is steeper over high elevations of the Sierra Nevada exceeding 7.7 °C km^{-1} on dry lightning days (figure 3(C)). MTLR is enhanced compared to climatology regionwide (figure 3(I)), indicating that enhanced mid-tropospheric instability relative to climatology is a key ingredient of dry lightning across the domain.

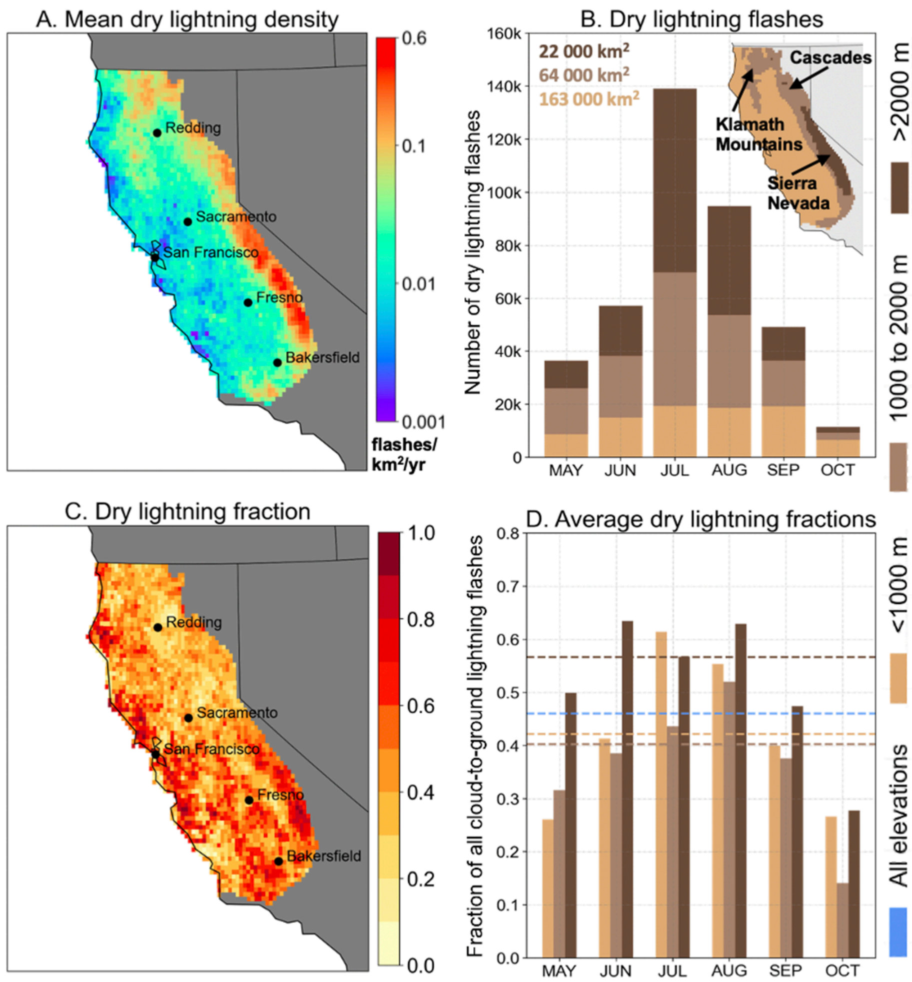

Figure 2. (A) Density of dry lightning flashes (cloud-to-ground lightning with <2.5 mm rainfall) averaged over May–October 1987–2020 (flashes km^{-2} yr^{-1}). (B) Total number of dry lightning flashes across three elevation zones (<1000 m, 1000–2000 m, >2000 m) within the domain for each month between 1987–2020. Text indicates the area of each elevation zone, and inset map shows the geographic distribution of the elevation zones and major mountain ranges. Fraction of all cloud-to-ground lightning flashes occurring as dry lightning in (C) each 0.1° NLDN grid cell across all months and (D) the three elevation zones for each month (bars). Dashed lines in (D) indicate the dry lightning fraction averaged across all months for each zone. Blue dashes in (D) represent the dry lightning fraction computed from all months and elevation zones. Note that values in (A) are presented on a base-10 logarithmic scale.

Mid-tropospheric specific humidity ($Q_{700-500}$) is highest over southern areas (figure 3(D)) and above background climatology on dry lightning days regionwide, with the largest enhancement of anomalies (>2 g kg^{-1}) in the coastal zone and southern areas (figure 3(J)). These areas largely correspond to the zone of enhanced UV_{500} (figure 3(G)) which could suggest increased mid-tropospheric moisture transport to the region by stronger atmospheric flow at that level. The dewpoint depression at 850 hPa (DD_{850}) is greater over the coastal zone with values exceeding 16 °C, indicating drier lower-tropospheric conditions compared to interior locations (figure 3(E)). However, DD_{850} is suppressed relative to climatology across the domain indicating increased atmospheric moisture content compared to climatology in the lower troposphere as well (figure 3(K)). Our results emphasize the importance of atmospheric moisture enhancement in the mid- to lower-troposphere on dry lightning days across the region. These results further suggest that even though the lower-troposphere is 'moistened' compared to normal on dry lightning days, conditions are not moist enough for substantial precipitation at the surface. Surface temperatures (T_{max}) on dry lightning days are similar to climatology, with the warmest temperatures over the Central Valley (figure 3(F)).

To understand the differences in meteorology during dry and wet lightning, we contrast the magnitude of these variables on dry versus wet lightning days. On dry lightning days, UV_{500} is generally weaker compared to wet lightning days across the domain with some areas experiencing reductions of >3 m s^{-1} (figure 3(M)), indicating that stronger mid-tropospheric flow is present on wet lightning days in many areas. This may suggest that large-scale atmospheric patterns with weaker mid-tropospheric winds but sufficient moisture, such as northward-displaced high pressure ridges centered over the Northwest or closed lows

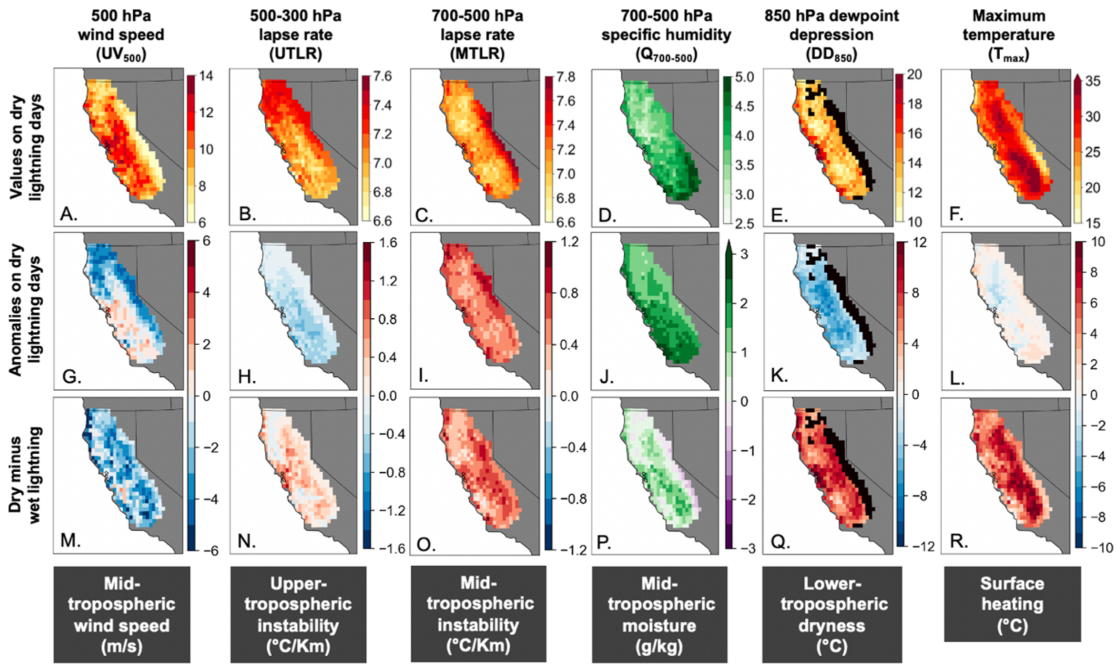

Figure 3. (A)–(F) Meteorological variables on dry lightning days at each 0.25° ERA5 grid cell during May–October 1987–2020. (G)–(L) Difference between values on dry lightning days and local background climatology, computed as the departure from the seven day running mean (1987–2020) centered on each dry lightning day at each grid cell. (M)–(R) Difference between values on dry lightning (<2.5 mm rainfall) and wet lightning days (≥2.5 mm rainfall). Black shading in (E, K, Q) indicates surface elevations above 850 hPa.

centered over California (van Wagtendonk and Cayan 2008, Abatzoglou 2016), may cause more dry lightning days compared to wet lightning days during the warm season. Conversely, UTLR is steeper on dry lightning days in many areas compared to wet lightning (figure 3(N)), despite suppressed UTLR compared to background climatology apparent in figure 3(H). $Q_{700-500}$ is also higher compared to wet lightning over many parts of the Central Valley, indicating a greater enhancement of mid-tropospheric moisture on dry lightning versus wet lightning days over many low-elevation areas (figure 3(P)). These results may be counterintuitive and could reflect a narrower atmospheric moisture layer on dry lightning days confined to the mid-troposphere, compared to a more saturated lower troposphere (below 700 hPa) associated with wet lightning (Wallmann *et al* 2010, Nauslar *et al* 2013). Conversely, $Q_{700-500}$ is reduced on dry lightning days over several mountainous areas compared to wet lightning, including over the Klamath Mountains and Sierra Nevada (figure 3(P)). While these results may indicate less available moisture, they may also reflect uncertainty in the exact location of moisture in the atmospheric column during dry lightning, which varies vertically from event to event, or instances when cloud bases are substantially above 700 hPa, which would not be resolved by a layer-average from 700 to 500 hPa (Wallmann *et al* 2010, Nauslar *et al* 2013).

Enhancements of mid-tropospheric instability, lower-tropospheric dryness, and surface heating are evident on dry- versus wet-lightning days across most of our study domain. MTLR is steeper on dry lightning versus wet lightning days regionwide with enhancements of >0.5 °C km^{-1} in central and southern areas (figure 3(O)), comparable to results of previous analyses over the interior West (e.g. Rorig and Ferguson 1999, 2002). DD_{850} and T_{max} are strongly enhanced, with large areas showing increases of >6 °C for both variables on dry versus wet lightning days (figures 3(Q) and (R)). Our findings demonstrate that considerably hotter and drier conditions exist in the lower troposphere when lightning occurs as dry across this region. These results agree with previous studies that reported significantly increased DD_{850} on dry versus wet lightning days over the northwest United States (Rorig and Ferguson 1999), northern Rockies (Rorig and Ferguson 2002), and southeastern Australia (Dowdy and Mills 2012b) sufficient to evaporate rainfall before it reaches the ground (i.e. 'virga'). Stronger surface heating, reflected by higher T_{max} across the domain compared to wet lightning days (figure 3(R)), contributes to enhanced lower-tropospheric dryness and greater mid-tropospheric instability congruent with previous studies (e.g. Rorig and Ferguson 1999, 2002).

We note that a limitation of our composite analysis is that we examine these variables in isolation and do not elucidate the concurrence of multiple variables initiating dry lightning. Wallmann *et al* (2010), for example, found that UTLR of >7.5 °C km^{-1} is an important indicator of dry lightning but only when combined with sufficient low- or mid-tropospheric moisture, and Rorig and Ferguson (1999) developed a dry lightning classification scheme that considered the 850–500 hPa lapse rate and DD_{850} simultaneously. More broadly, Nauslar *et al* (2013) showed that the most likely zones for dry lightning exist at the periphery of high-moisture and high-instability environments, where convection can produce dry lightning but without sufficient moisture to produce 'wetting' rain. A multivariate approach could improve our understanding of these relationships and help operational forecasters and fire management entities better anticipate dry lightning at longer lead-times than are currently available (Nauslar *et al* 2013).

3.3. Climatology of widespread dry lightning outbreaks

Widespread dry lightning days (dry lightning in >6.1% of the domain) have occurred throughout the warm season (figure 4(A)). Although the majority of these days occurred during July-August, the largest spatial extents occurred in June and September (figures 4(A) and (C)). Widespread dry lightning outbreaks, on average, occurred over higher elevations during May–August and lower elevations in September–October (figure 4(A), brown line). Figure 4(B) shows the largest one day (orange) and two day (red) dry lightning outbreaks, and the total number of widespread dry lightning days in each year (blue bars). There is substantial interannual variability in outbreak frequency and spatial extents. Two-day outbreak spatial extents affecting >20% of the domain have occurred in 8 of these years (1987, 1988, 1990, 1991, 2003, 2008, 2017 and 2020; figure 4(B)). Some observational uncertainty exists in the early part of the record due to lower detection efficiency of the NLDN network, particularly before a major network upgrade in 1995 (Cummins and Murphy 2009). Nonetheless, we find frequent widespread dry lightning days and large spatial extents of dry lightning between 1987 and 1995. In contrast, relatively few widespread dry lightning days have occurred since 2015 (figure 4(B), blue bars).

The largest lightning-caused wildfire outbreaks, measured by burned area, started on or around 31 August 1987 (∼260 000 ha), 21 June 2008 (∼352 000 ha), and 17 August 2020 (987 000 ha), which were also three of the ten most widespread dry lightning days (figure 4(C)). The 'Siege of 1987' wildfire outbreak (Duclos *et al* 1990) resulted from four consecutive days of widespread dry lightning (30 August–2 September) peaking at 16.4% of the domain on 31 August over mainly forested regions of the Sierra Nevada, Cascades, and Klamath Mountains (figure 4(C)). The 'exceptional' dry lightning outbreak of 21 June 2008 represents the largest single-day spatial extent of 25.1% and affected a large swath of northern California (figure 4(C)) (Wallmann *et al* 2010), resulting in the 8th largest lightning-caused fire over this domain in the 34 year record (Basin Complex, ∼66 000 ha). The dry lightning outbreak of 16–17 August 2020 ignited the August Complex, SCU Lightning Complex, LNU Lightning Complex, and North Complex fires—the 1st, 4th, 6th, and 7th largest fires on record in California—contributing to the state's largest annual burned area in modern records (Keeley and Syphard 2021). The two day outbreak together affected ∼25.7% of the domain even though the individual daily spatial extents were less remarkable peaking at 15.2% on 17 August (figures 4(B) and (C)). Notably, the 2008 and 2020 outbreaks represented the only widespread dry lightning days in their respective years (figure 4(B), blue bars), emphasizing the importance of rare but extreme dry lightning outbreaks as drivers of extreme wildfire episodes in this region.

We test the sensitivity of our dry lightning climatology to our choice of precipitation dataset by comparing key climatological characteristics identified above using gridMET with the climatology created using the Multi-Source Weighted Ensemble Precipitation (MSWEP) V2.8 dataset (Beck *et al* 2019) at a 0.1° resolution (www.gloh2o.org/mswep/; 1979–present). MSWEP combines precipitation data from surface gauges, satellites, and reanalysis. Compared to other high spatial and temporal resolution multi-source precipitation datasets, MSWEP is available for the entire analysis period. Daily precipitation totals provided by MSWEP are binned 5 PM–5 PM local time and thus match the temporal aggregation of the NLDN data. Although gridMET and MSWEP are created from different data sources and over different daily timesteps, the spatial patterns of mean lightning density and dry lightning fraction and monthly differences in dry lightning characteristics at different elevations are generally similar over 1987–2020 (figures S.5–S.7). A notable difference is the larger dry lightning fraction over northeastern areas when using MSWEP (figure S.5(D)), which could result from different temporal aggregation in these datasets or differences in input data sources. Additionally, the coarser spatial resolution of MSWEP compared to gridMET might lead to averaging of sub-grid rainfall over each grid point, possibly causing more grid points to fall below the dry lightning threshold (<2.5 mm). Although MSWEP may be expected to capture more precipitation than the gauge-based gridMET over sparsely-gauged regions (e.g. Sierra Nevada), the accuracy of satellite and reanalysis precipitation inputs in the presence of dry sub-cloud environments that lead to virga is unknown. In addition, the widespread dry lightning days are largely consistent between the two datasets, with slight differences in the identified extents.

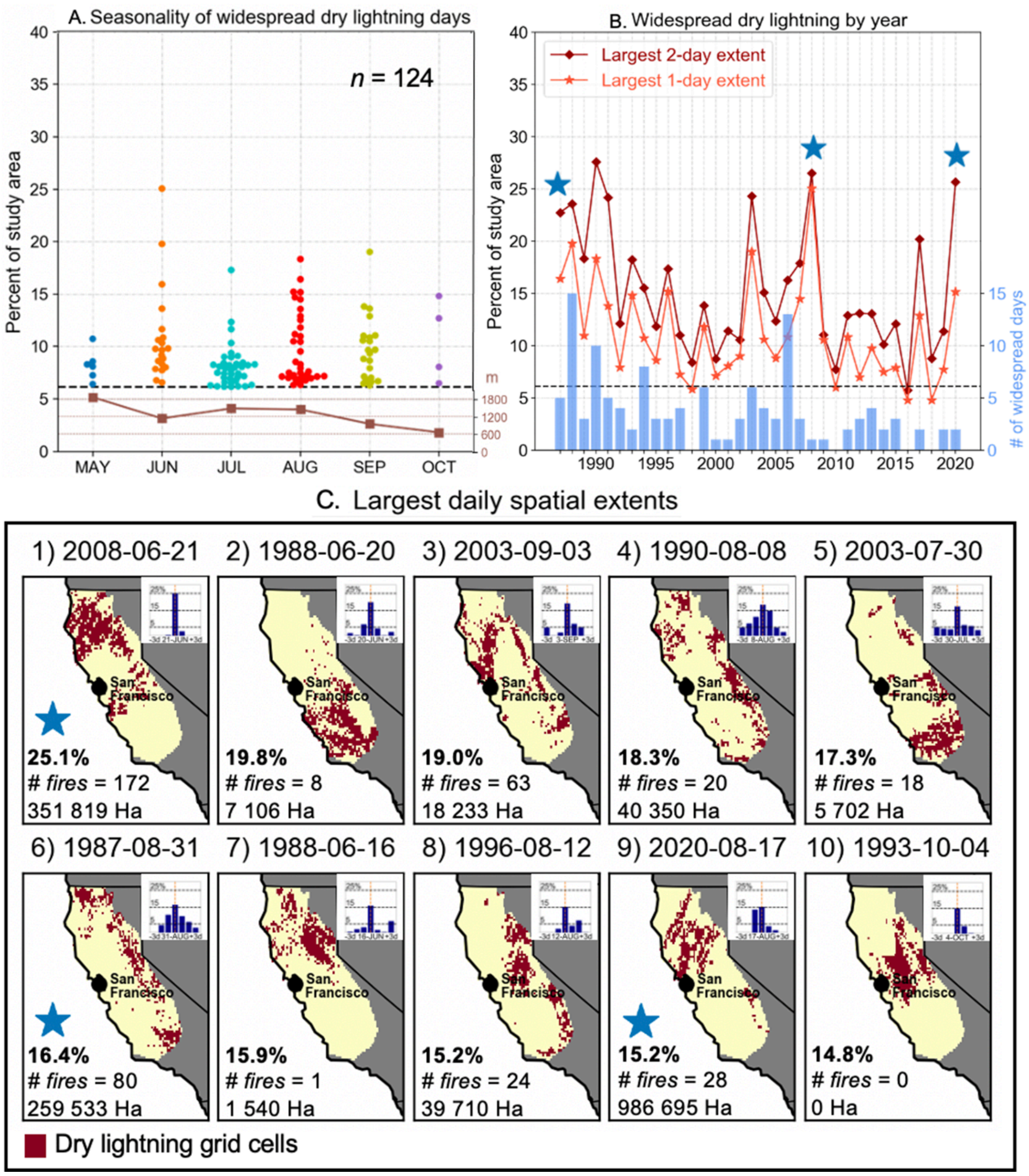

Figure 4. (A) Monthly distribution of the 124 widespread dry lightning days (dry lightning in >6.1% of all 0.1° NLDN grid cells) between May–October 1987–2020 and median elevation of affected grid cells on these days (brown line). (B) Maximum annual dry lightning extent (percentage of all grid cells in domain) defined over one day (orange) and two day (red) periods. For two day periods, only unique grid cells are counted. Data points in (A) are jittered for visualization within each month. In (A) and (B), dashed black line represents the fraction of grid cells (6.1%) corresponding to the 95th percentile of all daily spatial extents of dry lightning over the 34 year period. Blue bars in (B) show the number of widespread dry lightning days defined at this threshold in each year. (C) Top-10 largest daily spatial extents of dry lightning over the study period. In (C), bold inset text indicates the percentage of grid cells experiencing dry lightning on that day, and inset bar charts show the daily spatial extents of dry lightning in the seven day window centered on that day. Other inset text shows the number of associated lightning-caused wildfires ignited during the seven day period and the final burned area from such fires (see section 2) from CAL FIRE. Blue markers in (B) and (C) denote widespread dry lightning outbreaks discussed in the text.

3.4. Clustering of large-scale atmospheric patterns on widespread dry lightning days

We identify four main types of weather patterns associated with dry lightning outbreaks in different parts of the domain. Figure 5 shows the four clusters representing the large-scale atmospheric patterns on widespread dry lightning days, their associated meteorological conditions, and the spatial patterns of dry lightning likelihood across the region. All clusters exhibit mid-tropospheric high-pressure ridging centered over different portions of the western North American continental interior (as indicated by higher values of 500 hPa geopotential heights (Z_{500}), figures 5(A)–(D)).

Cluster 1 features a strong ridge over the continental interior, with offshore troughing likely providing dynamic lifting and enhancing mid-tropospheric moisture transport to the region, particularly if tropical

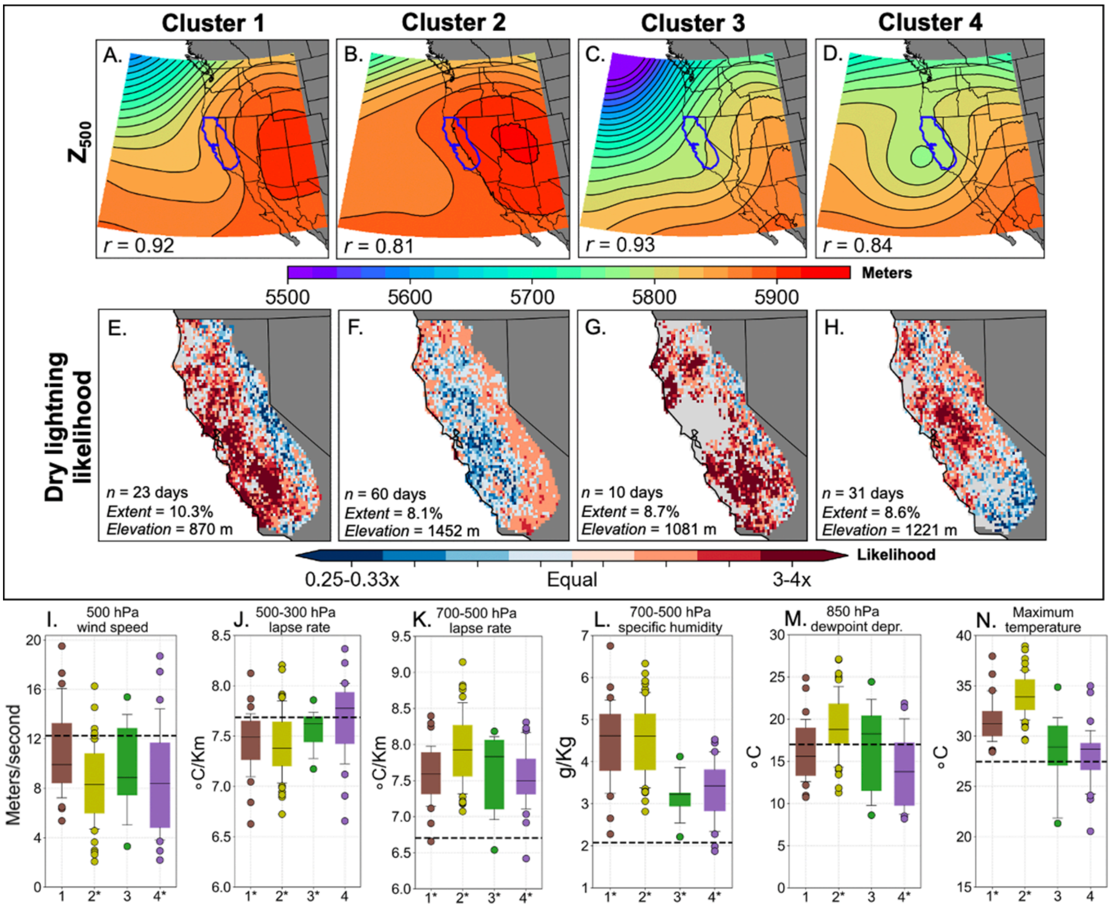

Figure 5. (A)–(D) *k*-means clusters of 500 hPa geopotential heights (Z_{500}) on widespread dry lightning days during May–October 1987–2020 ($n = 124$). The domain outline is shown in blue. Inset text indicates median 2D pattern correlation (r) between the cluster's composite and constituent daily patterns. (E)–(H) Dry lightning likelihood in each grid cell associated with that cluster's Z_{500} pattern, relative to random chance. For example, dark red shading indicates that on widespread dry lightning days, these grid cells are >3 times more likely to experience dry lightning with that cluster's Z_{500} pattern compared to random chance. Light gray shading denotes grid cells which have not been constituent to a widespread dry lightning day with that cluster. (I)–(N) Boxplots of domain-averaged meteorological variables on widespread dry lightning days for each cluster. Asterisks next to cluster names denote significant difference ($P < 0.05$) of that cluster's distribution compared to all non-widespread days (dry lightning in <6.1% of domain including no dry lightning) in the 34 year record according to a Kolmogorov–Smirnov test. Inset text in (E)–(H) shows the number of days assigned to each cluster and the median extent and elevation of all grid cells affected on widespread dry lightning days in that cluster. Dashed lines in (I)–(N) indicate the domain-averaged value of each variable on non-widespread days.

moisture is readily available over the eastern Pacific Ocean (figure 5(A)). For example, the August 2020 dry lightning outbreak—a cluster 1 pattern—developed after the circulation of an approaching shortwave trough interacted with Tropical Storm Fausto in the eastern tropical Pacific (Blake 2021), sending large amounts of mid-tropospheric moisture northward over California that was sufficient to initiate widespread elevated convection. Cluster 1 is associated with increased dry lightning likelihood throughout the domain outside of the Sierra Nevada, the largest median dry lightning spatial extent (∼10.3%), and the lowest median elevation of dry lightning (870 m, figure 5(E)). Cluster 2 shows a broad, amplified ridge extending over the Pacific coastal states northward to Canada (figure 5(B)). This pattern is associated with enhanced dry lightning likelihood over the Sierra Nevada and the highest median elevation of dry lightning (1452 m, figure 5(F)). Cluster 3 shows weaker ridging over the continental interior and strong, amplified troughing offshore centered over the northeast Pacific Ocean (figure 5(C)) with enhanced dry lightning likelihood everywhere except the central parts of the domain (figure 5(G)). Cluster 4 is a 'closed low' pattern (figure 5(D)) and corresponds to enhanced dry lightning likelihood in northern and central areas of the domain with decreased likelihood in southern areas (figure 5(H)).

The large-scale atmospheric flow represented by clusters 1 and 3—with ridging in the continental interior and troughing offshore—resembles the 'transitional' weather pattern following high pressure ridge breakdown identified by previous studies as favorable for warm-season lightning outbreaks over broad areas of the western United States (figures 5(A) and (C)) (e.g. Abatzoglou and Brown 2009, Werth and Ochoa 1993, Dettinger *et al* 1999, Rorig and Ferguson 1999, Kalashnikov *et al* 2020). These patterns are conducive to shortwave troughs transiting the region from west to east, which have produced some of the most widespread dry lightning outbreaks over northern California including both the 2008 (cluster 3) and 2020 (cluster 1) outbreaks (Wallmann *et al* 2010, Nauslar *et al* 2013). In contrast, cluster 2 does not produce widespread dry lightning outbreaks over many lowland areas (figure 5(F)). Rather, this is a common summertime lightning pattern over mainly high terrain during the North American Monsoon season, as northward extension of ridging over the coastal states promotes monsoonal moisture transport, which combines with orographic lifting to initiate convection over mountains (figure 5(B)) (Abatzoglou and Brown 2009, Kalashnikov *et al* 2020). Indeed, cluster 2 accounts for 60 of the 124 observed widespread dry lightning days (figure 2(F)), and 50 of these days occurred during July–August representing peak monsoon season (figure S.8(B)). The dry lightning outbreak of 31 August 1987 is an example of a cluster 2 pattern, affecting mainly areas over high terrain (figure 4(C)).

Domain-averaged meteorological variables further illustrate the dynamic (figure 5(I)) and thermodynamic (figures 5(J)–(N)) conditions associated with each cluster. Cluster 1, associated with the most widespread median dry lightning spatial extent and occurring at the lowest elevations (figure 5(E)), features the strongest average UV_{500} among all clusters of $\sim$9.9 m s^{-1} (figure 5(I)), supporting the earlier finding of stronger mid-tropospheric winds on dry lightning days in these areas compared to higher elevations. The median UTLR values associated with Clusters 1–3 range from 7.4 to 7.6 °C km^{-1} and are below the climatological average of 7.7 °C km^{-1} computed from all other days (figure 5(J)), while Cluster 4 has the highest median ULTR of 7.8 °C km^{-1}. All clusters show significant enhancement of MTLR and $Q_{700–500}$ compared to background climatology (figures 5(K) and (L)), reinforcing the importance of increased mid-tropospheric instability and moisture in promoting widespread dry lightning outbreaks across this region irrespective of the synoptic configuration. Cluster 2, associated with a strong ridge of high pressure over the coastal states and the highest median elevation of dry lightning risk, exhibits the largest values of MTLR, $Q_{700–500}$, DD_{850} and T_{max} (figures 5(K)–(N)) yet shows decreased dry lightning likelihood in most of the low-elevation areas (figure 5(F)). This suggests the importance of atmospheric features associated with the other three clusters in causing dry lightning over lower elevations, including troughing (clusters 1 and 3) and closed lows (cluster 4; figures 5(A), (C)–(D)). These patterns can provide favorable mid-and upper-level dynamics, in addition to enhanced instability and moisture transport, to support warm-season convection over low-elevation areas, which lack orographic lifting and low-level forcing typically associated with thunderstorm development (Wallmann *et al* 2010, Nauslar *et al* 2013).

4. Summary and conclusions

In this study we have developed the first long-term and spatially contiguous climatology of dry lightning and examined its elevational dependence in central and northern California—a highly populated region that has experienced numerous destructive lightning-caused wildfires in recent decades. We identify local and large-scale meteorological conditions associated with such dry lightning outbreaks. Our work builds on previous studies of individual dry lightning outbreaks (e.g. Wallmann *et al* 2010, Nauslar *et al* 2013) and distinguishes the meteorological conditions associated with dry versus wet lightning. We demonstrate that dry lightning preferentially occurs at higher elevations and peaks during July-August, while lower elevations account for a larger proportion of dry lightning during September–October—representing a reversal of the relationship between dry lightning and elevation during the transition from summer to fall. We show that many low-elevation locations experience a large fraction of their lightning occurring as dry (versus wet) and experience a longer dry lightning season extending into fall (figures 2(B) and (C)). This is particularly important since both live and dead fuels tend to be extremely dry before the arrival of cool-season rains, further elevating the risk of wildfires late in the burning season (Court 1960, Balch *et al* 2018, Goss *et al* 2020).

We conduct a composite analysis of meteorological conditions on dry lightning days at each grid cell across the varied geography of this region. We show that two thermodynamically related variables—MTLR and $Q_{700–500}$—are consistently above background climatology across the region on dry lightning days (figures 3(I) and (J)), indicating that enhanced mid-tropospheric instability and moisture are key meteorological ingredients for dry lightning. Compared to wet lightning, we find that dry lightning occurs with considerably greater values of T_{max}, DD_{850}, and MTLR across the domain suggesting a much hotter, drier lower troposphere with greater mid-tropospheric instability when lightning occurs during dry versus wet thunderstorms (figures 3(P)–(R)). We find greater UV_{500} and $Q_{700–500}$ on dry lightning days over lower elevations, suggesting stronger mid-tropospheric steering flow and moisture enhancement in these parts of the domain compared to when dry lightning occurs over higher terrain. We also find steeper UTLR over northern areas, indicating greater upper-tropospheric instability on dry lightning days there compared to southern areas.

Widespread dry lightning outbreaks create the potential for multiple simultaneous wildfire ignitions that can severely impact fire suppression efforts due to the geographic dispersion of ignitions and the potential for substantial resource commitments. In this study, we present the first assessment of the climatology and spatial extents of these dry lightning outbreaks across this region. While the majority of widespread dry lightning days occurred in July–August consistent with overall dry lightning climatology, they also occurred throughout the warm season with the largest spatial extents observed in June and September, respectively (figure 4(A)). Although vegetation, antecedent climate, and post-ignition weather conditions modulate wildfire extent, the largest lightning-caused wildfire burned areas in the 34 year record nonetheless resulted from widespread dry lightning outbreaks centered on 31 August 1987, 21 June 2008, and 17 August 2020 (figure 4(C)). Our findings indicate that large dry lightning outbreaks can occur in otherwise 'quiet' years for dry-lightning activity as was demonstrated in 2008 and 2020, when some of the most widespread dry lightning days on record ignited numerous wildfires leading to costly and destructive wildfire seasons, despite a lack of any other widespread dry lightning days in those years (figures 4(B) and (C)). We identify four types of large-scale atmospheric patterns associated with widespread dry lightning outbreaks over this region. All four patterns are associated with different configurations of high pressure ridging over the continental interior, three of which additionally feature offshore troughing that provides a lifting mechanism and promotes moisture transport into the region (figures 5(A), (C) and (D)).

As our study domain is a highly populated region prone to lightning-caused wildfires, understanding the climatology and meteorology of dry lightning is critical for informing operational forecasts and climate model projections of dry lightning risk across the varied geography found here. Increased forecast accuracy of dry lightning outbreaks can aid fire suppression efforts, as firefighting resources can be strategically pre-positioned in at-risk areas. Finally, our findings regarding dry lightning are also relevant to efforts aimed at better constraining future risk of wildfire ignition in California from climate model projections—independent of changes to fire weather, biophysical factors, or human ignitions across this region.

Data availability statement

The data that support the findings of this study are openly available at the following URL/DOI: https://zenodo.org/record/6774536#.YsPexcHMLiy.

Acknowledgments

We thank two anonymous reviewers for their insightful comments that helped improve this paper. We acknowledge ECMWF's Copernicus Climate Change Service for providing ERA5 data, and Vaisala for collecting the NLDN lightning data used in this study. We sincerely thank Jim Wallmann for input regarding meteorological variables. This research used resources from the Center for Institutional Research Computing at Washington State University. D A K and D S were supported by NASA FINESST award 80NSSC21K1603. D L S was supported by a collaboration between the Institute of the Environment and Sustainability at the University of California, Los Angeles; the Center for Climate and Weather Extremes at the National Center for Atmospheric Research; and the Nature Conservancy of California. J T A was supported by NSF award OAI-2019762. D T was supported by the National Center for Atmospheric Research, which is a major facility sponsored by the National Science Foundation under Cooperative Agreement No. 1755088.

ORCID iDs

Dmitri A Kalashnikov https://orcid.org/0000-0002-2777-4909
John T Abatzoglou https://orcid.org/0000-0001-7599-9750
Daniel L Swain https://orcid.org/0000-0003-4276-3092
Deepti Singh https://orcid.org/0000-0001-6568-435X

References

Abatzoglou J T 2013 Development of gridded surface meteorological data for ecological applications and modelling *Int. J. Climatol.* **33** 121–31

Abatzoglou J T 2016 Contribution of cutoff lows to precipitation across the United States *J. Appl. Meteorol. Climatol.* **55** 893–9

Abatzoglou J T and Brown T J 2009 Influence of the Madden–Julian oscillation on summertime cloud-to-ground lightning activity over the continental United States *Mon. Weather Rev.* **137** 3596–601

Abatzoglou J T, Kolden C A, Balch J K and Bradley B A 2016 Controls on interannual variability in lightning-caused fire activity in the western US *Environ. Res. Lett.* **11** 045005

Abatzoglou J T and Williams A P 2016 Impact of anthropogenic climate change on wildfire across western US forests *Proc. Natl Acad. Sci.* **113** 11770–5
Balch J K, Bradley B A, Abatzoglou J T, Nagy R C, Fusco E J and Mahood A L 2017 Human-started wildfires expand the fire niche across the United States *Proc. Natl Acad. Sci.* **114** 2946–51
Balch J K, Schoennagel T, Williams A P, Abatzoglou J T, Cattau M E, Mietkiewicz N P and Denis L A 2018 Switching on the Big Burn of 2017 *Fire* **1** 9
Barbero R, Abatzoglou J T, Steel E A and Larkin N K 2014 Modeling very large-fire occurrences over the continental United States from weather and climate forcing *Environ. Res. Lett.* **9** 124009
Bartlein P J, Hostetler S W, Shafer S L, Holman J O and Solomon A M 2008 Temporal and spatial structure in a daily wildfire-start data set from the western United States (1986–96) *Int. J. Wildland Fire* **17** 8–17
Bates B C, Dowdy A J and Chandler R E 2017 Classification of Australian thunderstorms using multivariate analyses of large-scale atmospheric variables *J. Appl. Meteorol. Climatol.* **56** 1921–37
Beck H E, Wood E F, Pan M, Fisher C K, Miralles D G, van Dijk A I J M, McVicar T R and Adler R F 2019 MSWEP V2 global 3-hourly 0.1° precipitation: methodology and quantitative assessment *Bull. Am. Meteorol. Soc.* **100** 473–500
Bertram I and Mayr G J 2004 Lightning in the eastern Alps 1993–1999, part I: thunderstorm tracks *Nat. Hazards Earth Syst. Sci.* **4** 501–11
Blake E 2021 Tropical Storm Fausto national hurricane center tropical cyclone report (National Hurricane Center) p 8 (available at: www.nhc.noaa.gov/data/tcr/EP112020_Fausto.pdf)
Brey S J, Barnes E A, Pierce J R, Wiedinmyer C and Fischer E V 2018 Environmental conditions, ignition type, and air quality impacts of wildfires in the southeastern and western United States *Earth's Future* **6** 1442–56
Chen B and Jin Y 2022 Spatial patterns and drivers for wildfire ignitions in California *Environ. Res. Lett.* **17** 055004
Court A 1960 Thunderstorm frequency in Northern California *Bull. Am. Meteorol. Soc.* **41** 406–9
Cummins K L and Murphy M J 2009 An overview of lightning locating systems: history, techniques, and data uses, with an in-depth look at the U.S. NLDN *IEEE Trans. Electromagn. Compat.* **51** 499–518
Dettinger M D, Cayan D R and Brown T J 1999 Summertime intraseasonal and interannual lightning variations in the western United States *Proc. 24th Annual NOAA Climate Diagnostics and Prediction Workshop* (*Tucson, Arizona, 1–5 November 1999*) (available at: https://citeseerx.ist.psu.edu/viewdoc/download?doi=10.1.1.529.3401&rep=rep1&type=pdf)
Detzer J, Loikith P C, Pampuch L A, Mechoso C R, Barkhordarian A and Lee H 2020 Characterizing monthly temperature variability states and associated meteorology across southern South America *Int. J. Climatol.* **40** 492–508
Doswell C A III and Rasmussen E N 1994 The effect of neglecting the virtual temperature correction on CAPE calculations *Weather Forecast.* **9** 625–9
Dowdy A J 2020 Climatology of thunderstorms, convective rainfall and dry lightning environments in Australia *Clim. Dyn.* **54** 3041–52
Dowdy A J and Mills G A 2012a Atmospheric and fuel moisture characteristics associated with lightning-attributed fires *J. Appl. Meteorol. Climatol.* **51** 2025–37
Dowdy A J and Mills G A 2012b Characteristics of lightning-attributed wildland fires in south-east Australia *Int. J. Wildland Fire* **21** 521–4
Duclos P, Sanderson L M and Lipsett M 1990 The 1987 forest fire disaster in California: assessment of emergency room visits *Arch. Environ. Health Int. J.* **45** 53–58
Easterling D R and Robinson P J 1985 The diurnal variation of thunderstorm activity in the United States *J. Appl. Meteorol. Climatol.* **24** 1048–58
Goss M, Swain D L, Abatzoglou J T, Sarhadi A, Kolden C A, Williams A P and Diffenbaugh N S 2020 Climate change is increasing the likelihood of extreme autumn wildfire conditions across California *Environ. Res. Lett.* **15** 094016
Grotjahn R *et al* 2016 North American extreme temperature events and related large scale meteorological patterns: a review of statistical methods, dynamics, modeling, and trends *Clim. Dyn.* **46** 1151–84
Hantson S, Andela N, Goulden M L and Randerson J T 2022 Human-ignited fires result in more extreme fire behavior and ecosystem impacts *Nat. Commun.* **13** 2717
Hersbach H *et al* 2020 The ERA5 global reanalysis *Q. J. R. Meteorol. Soc.* **146** 1999–2049
Kalashnikov D A, Loikith P C, Catalano A J, Waliser D E, Lee H and Abatzoglou J T 2020 A 30-Yr climatology of meteorological conditions associated with lightning days in the interior western United States *J. Clim.* **33** 3771–85
Kalashnikov D A, Schnell J L, Abatzoglou J T, Swain D L and Singh D 2022 Increasing co-occurrence of fine particulate matter and ground-level ozone extremes in the western United States *Sci. Adv.* **8** eabi9386
Keeley J E and Syphard A D 2018 Historical patterns of wildfire ignition sources in California ecosystems *Int. J. Wildland Fire* **27** 781–99
Keeley J E and Syphard A D 2021 Large California wildfires: 2020 fires in historical context *Fire Ecol.* **17** 11
Komarek E V Sr 1967 The nature of lightning fires *Proc. 7th Tall Timbers Fire Ecology Conf.* pp 5–41 (available at: http://talltimbers.org/wp-content/uploads/2014/03/Komarek1967_op-1.pdf)
MacNamara B R, Schultz C J and Fuelberg H E 2020 Flash characteristics and precipitation metrics of western U.S. lightning-initiated wildfires from 2017 *Fire* **3** 19
MacQueen J 1967 Some methods for classification and analysis of multivariate observations *Proc. 5th Berkeley Symp. on Mathematical Statistics and Probability* vol 1 pp 281–97 (available at: https://digitalassets.lib.berkeley.edu/math/ucb/text/math_s5_v1_article-17.pdf)
Maddox R A, Canova F and Hoxit L R 1980 Meteorological characteristics of flash flood events over the western United States *Mon. Weather Rev.* **108** 1866–77
May R M *et al* 2021 MetPy: a python package for meteorological data *Unidata* (available at: https://github.com/Unidata/MetPy)
Miller J D, Skinner C N, Safford H D, Knapp E E and Ramirez C M 2012 Trends and causes of severity, size, and number of fires in northwestern California, USA *Ecol. Appl.* **22** 184–203
Moore B J, White A B and Gottas D J 2021 Characteristics of long-duration heavy precipitation events along the west coast of the United States *Mon. Weather Rev.* **149** 2255–77
Nauslar N, Kaplan M, Wallmann J and Brown T 2013 A forecast procedure for dry thunderstorms *J. Oper. Meteorol.* **1** 200–14
Parks S A and Abatzoglou J T 2020 Warmer and drier fire seasons contribute to increases in area burned at high severity in western US forests from 1985 to 2017 *Geophys. Res. Lett.* **47** e2020GL089858
Podschwit H and Cullen A 2020 Patterns and trends in simultaneous wildfire activity in the United States from 1984 to 2015 *Int. J. Wildland Fire* **29** 1057–71
Rochette S M, Moore J T and Market P S 1999 The importance of parcel choice in elevated CAPE computations *Natl Wea. Dig.* **23** 20–32 (available at: https://citeseerx.ist.psu.edu/viewdoc/download?doi=10.1.1.663.884&rep=rep1&type=pdf)

Rorig M L and Ferguson S A 1999 Characteristics of lightning and wildland fire ignition in the Pacific Northwest *J. Appl. Meteorol. Climatol.* **38** 1565–75

Rorig M L and Ferguson S A 2002 The 2000 fire season: lightning-caused fires *J. Appl. Meteorol. Climatol.* **41** 786–91

Rorig M L, McKay S J, Ferguson S A and Werth P 2007 Model-generated predictions of dry thunderstorm potential *J. Appl. Meteorol. Climatol.* **46** 605–14

Schultz C J, Nauslar N J, Wachter J B, Hain C R and Bell J R 2019 Spatial, temporal and electrical characteristics of lightning in reported lightning-initiated wildfire events *Fire* **2** 15 pp

Show S B and Kotok E I 1923 Forest fires in California from 1911–1920: an analytical study (U S Dep Agric Dep Circ) p 243 (available at: https://www.google.com/url?sa=t&rct=j&q=&esrc=s&source=web&cd=&ved=2ahUKEwj6tqLSy6b5AhWZATQIHYCPDacQFnoECAYQAQ&url=https%3A%2F%2Fir.library.oregonstate.edu%2Fdownloads%2Fst74cr83x&usg=AOvVaw3-2lBHxJsPFqKO5TSugrgp)

Soriano L J R, Pablo F D and Diez E L G 2001 Meteorological and geo-orographical relationships with lightning activity in Castilla-Leon (Spain) *Meteorol. Appl.* **8** 169–75

Tardy A 2001 Combining numerical model and observed soundings with VIL Density to forecast severe thunderstorms in the Sierra Nevada Western Reg Tech Attach No 01–05 (available at: www.weather.gov/media/wrh/online_publications/TAs/ta0105.pdf)

Tardy A 2002 The northern Sacramento Valley surface moisture convergence zone Western Reg Tech Attach No 02–07 (available at: www.weather.gov/media/wrh/online_publications/TAs/ta0207.pdf)

Taszarek M, Brooks H E, Czerneki B, Szuster P and Fortuniak K 2018 Climatological aspects of convective parameters over Europe: a comparison of ERA-Interim and sounding data *J. Clim.* **31** 4281–308

van Wagtendonk J W 1994 Spatial patterns of lightning strikes and fires in Yosemite National Park *Proc. 12th Int. Conf. on Fire and Forest Meteorology* Washington D C: American Meteorological Society pp 223–31

van Wagtendonk J W and Cayan D R 2008 Temporal and spatial distribution of lightning strikes in California in relation to large-scale weather patterns *Fire Ecol.* **4** 34–56

Visualization & Analysis Systems Technologies (VAST) 2021 Geoscience community analysis toolkit (GeoCAT-comp version 2021.5.1) [Software] (Boulder, CO: UCAR/NCAR—Computational and Informational System Lab) (available at: https://github.com/NCAR/geocat-comp)

Wallmann J, Milne R, Smallcomb C and Mehle M 2010 Using the 21 June 2008 California lightning outbreak to improve dry lightning forecast procedures *Weather Forecast.* **25** 1447–62

Werth P and Ochoa R 1993 The evaluation of Idaho wildfire growth using the Haines Index *Weather Forecast.* **8** 223–34

Williams A P, Abatzoglou J T, Gershunov A, Guzman-Morales J, Bishop D A, Balch J K and Lettenmaier D P 2019 Observed impacts of anthropogenic climate change on Wildfire in California *Earth's Future* **7** 892–910